A New Class of Ionic Liquids: Anion Amphiprotic Ionic Liquids

ARTICLE *in* JOURNAL OF PHYSICAL CHEMISTRY LETTERS · AUGUST 2012

Impact Factor: 7.46 · DOI: 10.1021/jz300752u

5 AUTHORS, INCLUDING:

Aleksandar Matic
Chalmers University of Technology
109 PUBLICATIONS **1,640** CITATIONS
SEE PROFILE

Patrik Johansson
Chalmers University of Technology
112 PUBLICATIONS **2,681** CITATIONS
SEE PROFILE

THE JOURNAL OF PHYSICAL CHEMISTRY Letters

Letter

pubs.acs.org/JPCL

A New Class of Ionic Liquids: Anion Amphiprotic Ionic Liquids

Marcel Treskow,[†] Jagath Pitawala,[†] Sven Arenz,[‡] Aleksandar Matic,[†] and Patrik Johansson*[,†]

[†]Department of Applied Physics, Chalmers University of Technology, SE-412 96 Gothenburg, Sweden

[‡]Department of Chemistry, University of Gothenburg, SE-412 96 Gothenburg, Sweden

ABSTRACT: We here present a new class of protic ionic liquids, anion amphiprotic ionic liquids (AAILs). These materials are protonation equilibrium free protic ionic liquids and interesting in their own right by not following the classical Brønsted acid−base neutralization concept. Due to the very simple synthesis route applied and their stable basic chemistry, we believe in a potential use for manifold applications. This is supported by the combination of practical material properties, foremost, a general intrinsic stability versus reversal of the formation reaction toward neutral species, broad liquidus ranges, long-term thermal stabilities, high conductivities, protic characteristics, and a general stability versus water.

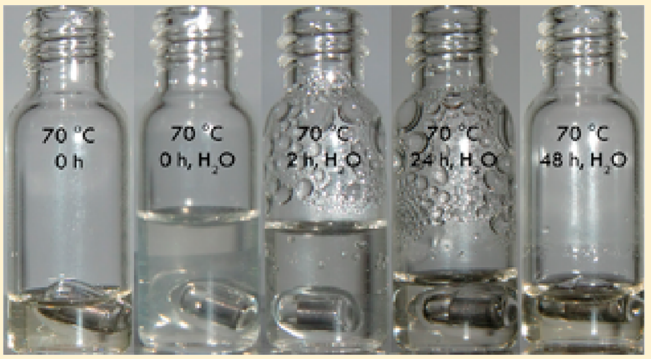

SECTION: Liquids; Chemical and Dynamical Processes in Solution

Protic ionic liquids (PILs) are today emerging as important materials[1] with an amazing diversity in properties and applications such as organic synthesis, chromatography, biological or fuel cell applications, explosives, or lubricants.[2] The subset of PILs is defined by the straightforward synthesis through the combination of a Brønsted acid and a Brønsted base. Here, we present a new class of PILs, anion amphiprotic ionic liquids (AAILs), PILs without a protonation equilibrium but rather based on the neutralization of basic methyl carbonate ionic liquids (ILs) with trifluoromethanesulfonamide ($CF_3SO_2NH_2$). This circumvents one of the major drawbacks of traditional PILs, the equilibrium between ionic and neutral species,[3,4] where the latter form might lead to material decomposition. As our materials are derived from an inert noncoordinating backbone structure, they can be made intrinsically stable at high temperatures,[5] and the easy path of synthesis opens for a variety of cations and anions to be applied while maintaining IL properties.

So far, PILs have been the reaction product between strong Brønsted acids and bases. The resulting equilibrium between charged and neutral species led to discussions about the necessary ΔpK_a between the acid and base to obtain an ionic degree > 99%, a level deemed necessary for a true IL.[6] These traditional PILs can be viewed as the first generation of ILs, where the proton is more or less strongly bonded to nitrogenous bases like primary, secondary, or tertiary amines, imidazole, caprolactame, or guanidine derivatives, or any other nitrogen-containing heterocycle.[2] Only a few examples of PILs with inorganic acid anions such as $H_2PO_4^-$ and HSO_4^{-7} have indicated another, second route, pointing to a second generation. The anion amphiprotic ILs presented here (Scheme 1) are the first examples with organic anions (even if $CF_3SO_2NH_2$ is indeed on the borderline to inorganic), which in turn promises easy access to different AAILs by using different amides or polyprotic acids in general. We stress that the AAILs have no acidic protons available and are not acidic compared to Brønsted acidic ILs, where always an additional acidic function is to be found, and the deprotonation would create a very weak corresponding base, the AAILs presented here have only an anion N−H proton, and its removal would create an extremely strong base.

Scheme 1. (a) Synthesis Scheme for AAILs and (b) Ions Used in This Work

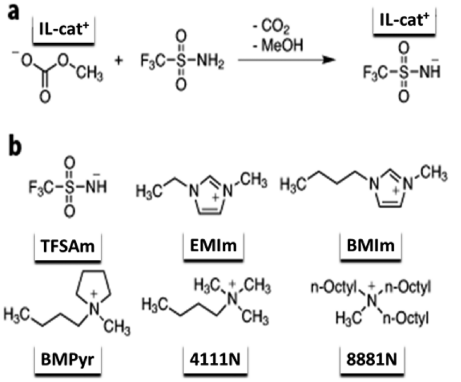

The key to protonation equilibrium free PILs with acidic protons are aprotic IL cation salts of diacids or amides. The AAILs presented here are all prepared by straightforward anion−anion neutralization reactions, starting from IL cation methylcarbonate and trifluoromethanesulfonamide (TFSAm). The synthesis method used is already well-established for

Received: June 11, 2012
Accepted: July 24, 2012

   dx.doi.org/10.1021/jz300752u | J. Phys. Chem. Lett. 2012, 3, 2114−2119

aprotic ILs[8,9] but has, to the best of our knowledge, never before been used to rationally obtain PILs. The reaction pathways and the obtained ILs are all shown in Scheme 1. We here focus on the smallest derivatives of the fluorinated sulfonamides in combination with different organic IL cations such as ethylmethylimidazolium (EMIm), butylmethylimidazolium (BMIm), butylmethylpyrrolidinium (BMPyr or Pyr_{14}), trioctylmethylammonium (8881N), and butyltrimethylammonium (4111N), all with promise of high conductivities. Ion size as well as any ion association will affect the ionic conductivity,[10] and, in particular, PILs with more delocalized charges and less ion interaction will have higher conductivities.

All of our AAILs show overall high conductivities above their phase transitions to liquids, Figure 1a. The conductivities at 20

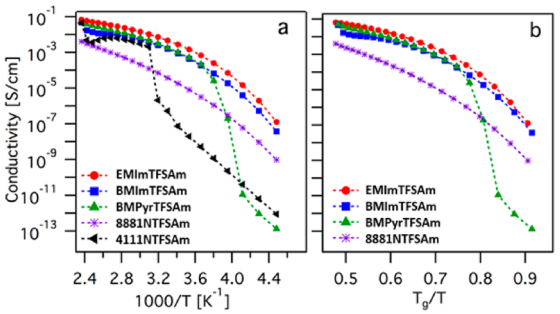

Figure 1. (a) Arrhenius plot of ionic conductivity versus temperature. (b) T_g/T scaled.

°C are between 4.5 mScm^{-1} for EMImTFSAm and 0.01 mScm^{-1} for 8881NTFSAm. A conductivity level of 10 mScm^{-1} is reached for all materials at ∼100 °C, and EMImTFSAm and BMImTFSAm reach this already at 50 °C. Comparing these values with related triflate (OTf) ILs, such as EMImTFSAm, to the PIL EImOTf[11] (10 mScm^{-1}) as well as the aprotic ILs EMImOTf and EMIm$(CF_3SO_2)_2N$ (7.7 and 7.6 mScm^{-1}),[12] our conductivities are only slightly lower. Thus, TFSAm can be considered as a rather weakly coordinating anion.

The temperature dependence of the ionic conductivity for all AAILs follows a non-Arrhenius behavior, as has been observed for other ILs, Figure 1a.[3,13] For 4111NTFSAm and BMPyrTFSAm, a sharp drop in the conductivity is observed at ∼40 and ∼−20 °C, respectively, as a result of crystallization. Above ∼130 °C, there is an unexpected decrease in the conductivity for 4111NTFSAm. In the same temperature range, the conductivity still increases for the BMIm-based AAIL, but it is less than expected by extrapolation. As the data are obtained from cooling curves, this behavior cannot be due to any IL decomposition, furthermore supported by overlap of subsequently recorded heating traces (not shown), and is therefore most likely related to a reversible, yet unknown minor structural change, affecting the ion dynamics.

In order to further investigate the structural dynamics origin of the conductivity, the data are plotted with a glass transition temperature (T_g/T)-scaled axis in Figure 1b (see also Table 1). The 4111NTFSAm has no observable T_g and is thus not included. It has previously been reported that a common master curve can be found in this representation, at least within a given cation family.[13,14] However, the AAILs do not fall on a common curve; thus, the differences in conductivity cannot solely be accounted for by T_g differences. It also shows the AAILs to have different fragilities, that is, the temperature dependence of the conductivity is different. Furthermore, the

Table 1. Thermal Properties for the TFSAm-Based AAILs

	EMIm	BMIm	BMPyr	4111N	8881N
T_g [°C]	−71	−69	−69		−71
T_m [°C]		17	16	56	11
T_d [°C][a]	238	237	201	198	194

[a]TGA temperature with 5% weight loss at 5 K/min.

conductivity does not drop dramatically with increased cation/anion radii. Still, however, the most conducting AAIL has the smallest cation, and the least conductive has the largest cation.

To further investigate the microscopic transport mechanism in the AAILs, we performed ^{1}H and ^{19}F PFG-NMR with DOSY experiments (Figure 2).[15] To obtain sufficiently high ion

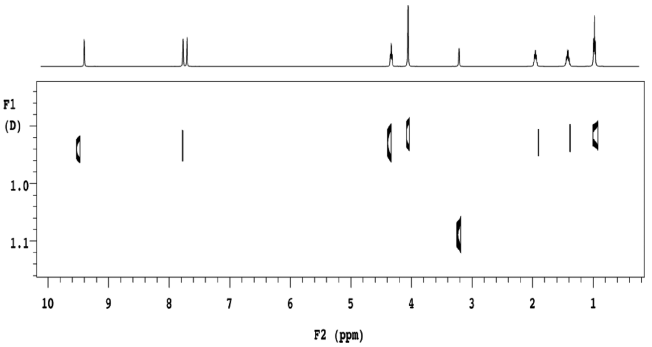

Figure 2. ^{1}H NMR DOSY of BMImTFSAm at 80 °C.

mobilities, the data were recorded at 80 °C. Below this temperature, the viscosities were too high to measure DOSY spectra, even with the highest possible probe gradient. From these experiments, we can disentangle the motion of the cations, anions, and possibly the anion N−H protons (Table 2). The proton transport in AAILs can, as for any PIL, occur by

Table 2. ^{1}H and ^{19}F Diffusion Coefficients (10^{-10} m^2 s^{-1}) of TFSAm-Based AAILs at 80 °C by DOSY PFG-NMR

	D_{C-H}	D_{N-H}	D_F	D_{N-H}/D_F
EMIm	1.5	1.4	1.2	1.17
BMIm	0.9	1.1	0.9	1.22
BMPyr	0.8	1.6	0.8	2.00
4111N	0.6	0.8	0.6	1.33
8881N	0.2	0.6	0.2	3.00

two mechanisms, diffusion transport by a vehicular mechanism and/or by a proton hopping Grotthuss-type mechanism.[16] Often, PILs have no significant proton mobility increase compared to the vehicular mobility of the constituent IL ions.[17] As can be seen in Table 2, the anions and cations are moving more or less with the same speed, and the trend in the diffusion coefficients agrees well with the conductivity data.

Comparing the diffusion coefficients for the anion and the N−H proton, we find that the mobility of the proton is higher for all AAILs, that is, the proton mobility is at least partially decoupled from the anion motion. For the BMPyrTFSAm and 8881NTFSAm AAILs, it is a remarkable factor of 2 and 3 higher (Table 2), clearly demonstrating their protic character.[18] Thus, to speculate, a Grotthuss mechanism[19,20] contributes to the proton mobility, with jumps between the anions. Here, the self-dissociation, from the $R-NH^-$ anion to $R-N^{2-}$ and $R-NH_2$, provides excess protons and free coordination partners.

dx.doi.org/10.1021/jz300752u | J. Phys. Chem. Lett. 2012, 3, 2114−2119

The double anion, $R-N^{2-}$, has its high charge density stabilized due to a mesomeric distribution of the charge.[21] The $R-NH^-$ anion can by this act like the amphoteric (and amphiprotic) water. In AAILs, in stark contrast to the most common solvent water, which needs to rotate a lone pair toward a proton,[20] the six lone pairs of the sulfonamide anion are, in close relation to, for example, phosphoric acid, already shell-like-distributed. With only a single available proton, a 3-D hydrogen network, like in water or H_3PO_4, is rather unlikely, but instead, two-dimensional chains are more probable. Within the AAILs, proton jumps can occur between the anions along such chains and be followed by local molecular rearrangements. Further support for the proposed proton-transport mechanism can be found in the ^{1}H NMR spectra where the peak shape of the N–H line at 80 °C is significantly broadened compared to that at 25 °C, indicative of a proton exchange increase, whereas the $N-CH_3$ peak is sharpened, being an internal reference and due to reduced viscosity (Figure 3).

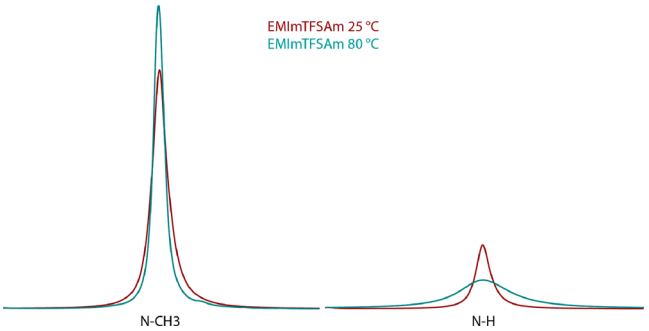

Figure 3. Peak shape of the N–H and $N-CH_3$ signals in ^{1}H NMR at 80 and 25 °C.

A wide liquidus range is found for all AAILs from the DSC experiments. All AAILs are easily supercooled, and for EMImTFSAm, no melting point could be obtained. The obtained T_g values are found at around −70 °C for all materials and thus are almost cation-independent, in agreement with observations for other related ILs.[2,22] Because crystallization is mainly influenced by packaging efficiency and steric hindrances, it is not surprising that BMImTFSAm and BMImOTf[23] show identical melting points (17 °C). The 12 K higher melting point of BMPyrTFSAm (16 °C) compared to the aprotic BMPyrOTf analogue (4 °C)[24] is still explainable as due to the above effects.

To further evaluate the thermal properties and, in particular, the stability versus decomposition, TGA measurements were performed, first by simply heating the samples from room temperature to 400 °C (at a rate of 5 K/min). The imidazolium family (cations BMIm and EMIm) is stable up to ∼240 °C (Table 1 and Figure 4a), where ∼5% mass loss is reached. The quaternary ammonium salts, including the pyrrolidinium family, are less stable and decompose at ∼200 °C.

These observed stabilities, while rather high in temperature are, however, still lower than their closest protic relatives, the triflate family, where methylimidazolium triflate is stable up to 323.5 °C[25] and triethylammonium triflate is stable up to 312.5 °C.[25] That all of our AAILs have the same decomposition temperature within a given cation family indicates that the decomposition mechanism is similar. This is surprising because ILs generally have individual decomposition temperatures (and mechanisms), where the anion and cation classes do not strictly

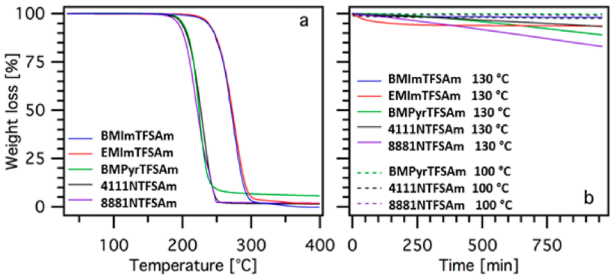

Figure 4. (a) TGA weight loss for heating to 400 °C at 5 K/min. (b) Isothermal TGA traces.

limit the stability.[2,22] In addition, all materials decomposed (>300 °C) to totally volatile reaction products, which requires charge neutrality for all species.

As the only possible decomposition mechanism for the ammonium species is the dealkylation reaction, the general decomposition pathway will most likely be an alkylation of the anion by the methyl group of the cation having the lowest steric hindrance (Scheme 2). Hence, the decomposition would first

Scheme 2. Suggested Decomposition Mechanism via Neutral Species

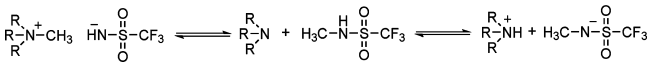

lead to a regular PIL, with proton equilibrium between alkylated charge-neutral sulfonamide and dealkylated nitrogen on the one hand and the IL obtained by acid–base equilibrium on the other hand. The ΔpK_a between these compounds is quite small, methylimidazoliumchloride with $\Delta pK_a = 7.1$[26] and *N*-methyltrifluoromethanesulfoneamide with $\Delta pK_a = 7.56$,[27] resulting in an equilibrium constant of $K = 1.06$. This enables also the back reaction and might further explain the conductivity changes observed above 130 °C (Figure 1a).

As a test of long-term stability, isotherms were recorded at 130 °C for 16 h (Figure 4b). The ammonium and pyrrolidinium families have significant weight loss at 130 °C, but long-term stability can be observed at 100 °C. A special observation is made for AAILs based on the imidazolium family. These have an initial mass loss, but this is most probably related to the decomposition of precursor impurities. The commercial methylcarbonate precursors used were synthesized via high-pressure autoclave synthesis, where a known side product is the replacement of the imidazolium ring protons with carbon dioxide, resulting in imidazolium carboxylates, which are thermally unstable and decompose under evolution of carbon dioxide under long-time exposure at high temperatures.[28] The here-obtained mass losses are in good agreement with the amount of impurities determined via the ^{1}H NMR analysis. As the mass losses are not caused by AAIL decomposition itself, it can rather be considered as a self-cleaning process. Thus, these AAILs are, in reality, thermally stable in the investigated temperature range.

From a practical point of view, stability toward water would be beneficial for general applicability of AAILs. In theory, an anion exchange to hydroxide is possible as the sulfonamide is in protonation equilibrium with water, leaving a hydroxyl IL. As a first test of the stability of our materials, we added 1.5 volume equivalent of water to BMImTFSAm and then annealed the solution at 70 °C for 48 h in an open glass vial (Figure 5a),

dx.doi.org/10.1021/jz300752u | J. Phys. Chem. Lett. 2012, 3, 2114–2119

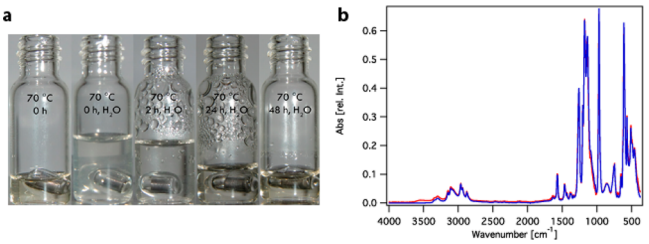

Figure 5. (a) A sample of BMImTFSAm during water evaporation. (b) BMImTFSAm ATR-IR spectra before (blue) and after (red) the water treatment.

slowly evaporating the water. In the end, there was no visible change in volume or color. ATR-IR spectra before and after water treatment prove the AAIL compound integrity by the congruency of the spectra in the fingerprint region (Figure 5b).

To conclude, we here show the first examples of a new class of ILs, AAILs. The synthesis route applied is simple, versatile, and uses a stable basic chemistry, opening the field for easy tuning of the properties. Their low melting points give a wide liquidus range and overall high conductivities, even at low temperatures, and, in addition, proton mobilities above the single ion diffusion speeds are detected by NMR diffusion measurements. Combining the conductivity values presented, the proton mobility and the thermal and water stability make our AAILs excellent targets for future experimental investigations as part of (nonaqueous) proton-exchange membrane fuel cells (PEMFC). In case the water solubility is unwanted or needs to be reduced, the ease of synthesis opens the possibility for creating more hydrophobic AAILs by using, for example, long-chain perfluorinated sulfonamide anions.

■ EXPERIMENTAL SECTION

Synthesis. AAILs were synthesized by stepwise addition of a stoichiometric amount of trifluoromethanesulfonamide (TFSAm) to a magnetically stirred solution of 50% methylcarbonate IL in MeOH at 45 °C (Scheme 1a). After the complete addition of sulfonamide (the evolution of CO_2 ceased), the reaction was stirred for an additional 2 h and cooled to RT. The solvent was removed under reduced pressure, and the obtained colorless liquids were dried for 18 h at 10^{-2} mbar and 60 °C, leaving the AAILs pure. The water content was determined by Karl Fischer titration to be less than 50 ppm in all samples. The yields were, in all cases, >99%. A full chemical characterization by ^{1}H, ^{13}C, and ^{19}F NMR, IR, DSC, and ESI-MS was made. The general purity of the materials was >99%, except for EMImTFSAm, which had a ∼5% impurity of carboxylated imidazolium derivatives.

Characterization. EMImTFSAm, slightly yellow liquid, T_g = −71.2 °C, T_m n.d., T_d = 237.8 °C. IR: 3341, 3294, 3107, 1665, 1573, 1509, 1453, 1390, 1325, 1260, 1203, 1177, 1133, 968, 848, 792, 744, 701, 649, 610, 565, 510, 487, 464. ESI-MS [m/z]: 111.1 (K^+), 147.9 (A^-). NMR [ppm] ^{1}H: 9.18 (s, 1 H), 7.79 (s, 1 H), 7.70 (s, 1 H), 4.19 (q, 2 H), 3.85 (s, 3 H), 2.53 (bs, 1 NH), 1.41 (t, 3 H); ^{13}C: 136.3, 123.6, 122.3 (q, 330 Hz), 122.0, 44.1, 35.6, 15.0; ^{19}F: −80.0 s. BMImTFSAm, colorless liquid, T_g = −69.3 °C, T_m = 16.5 °C, T_d = 236.8 °C. IR: 3339, 3295, 3106, 2963, 2877, 1572, 1466, 1383, 1259, 1204, 1177, 1135, 969, 859, 744, 653, 610, 566, 511, 457. ESI-MS [m/z]: 139.1 (K^+), 147.9 (A^-). NMR [ppm] ^{1}H: 9.17 (s, 1 H), 7.78 (s, 1 H), 7.71 (s, 1 H), 4.16 (t, 2 H), 3.85 (s, 3 H), 2.93 (bs, 1 NH), 1.76 (quint, 2 H,) 1.26 (sext, 2 H,), 0.90 (t, 3 H); ^{13}C: 136.6, 123.6, 122.3, 122.2 (q, 330 Hz), 48.5, 35.7, 31.4, 18.8, 13.3; ^{19}F: −80.0 s. BMPyrTFSAm, slightly yellow liquid, T_g −69.2 °C, T_m 16.4 °C, T_d 200.7 °C, IR: 3342, 3294, 2965, 2878, 1467, 1259, 1202, 1175, 1131, 1082, 1005, 967, 929, 825, 742, 611, 565, 510, 456. ESI-MS [m/z] 142.2 (K^+), 147.9 (A^-) NMR [ppm] ^{1}H 3.55−3.35 (m, 4 H), 3.35−3.25 (m, 2 H), 3.0 (s, 3 H), 2,44 (bs, 1 NH) 2.15−2.10 (m, 4 H,) 1.68 (quint, 2 H), 1.31 (sext, 2 H), 0.93 (t, 3 H), ^{13}C 122.3 (q, 330 Hz), 63.4, 62,8 47.4, 24.9, 21.0, 19.3, 13.5, ^{19}F −79.9 s. 4111NTFSAm, colorless solid, T_g n.d., T_m = 56 °C, T_d =198.4 °C. IR: 3343, 3301, 3034, 2966, 2879, 1668, 1483, 1422, 1257, 1202, 1176, 1133, 967, 910, 743, 612, 566, 511, 453. ESI-MS [m/z]: 116.1 (K^+), 147.9 (A^-). NMR [ppm] ^{1}H: 3.28 (t, 2 H), 3.03 (s, 9 H), 2.47 (bs, 1 NH), 1.70−1.60 (m, 2 H,) 1.37−1.25 (m, 2 H,), 0.93 (t, 3 H); ^{13}C: 122.8 (q, 330.47 Hz), 65.5, 52.5, 24.4, 19.6, 13.8; ^{19}F: −79.9 s. 8881NTFSAm, slightly brown liquid, T_g = −70.6 °C, T_m = 10.9 °C, T_d = 193.6 °C. IR: 3346, 2955, 2924, 2856,1467, 1264, 1203,1175, 1138, 1078, 969, 723, 612, 566, 512, 450. ESI-MS [m/z]: 368.4 (K^+), 147.9 (A^-). NMR [ppm] ^{1}H: 3.30−3.15 (m, 6 H), 2.97 (s, 3 H), 2.41 (bs, 1 NH), 1.75−1.55 (m, 6 H) 1.42−1.20 (m, 30 H), 0.97−0.85 (m, 9 H); ^{13}C: 123.2 (q, 330 Hz), 64.4, 48.4, 32.0, 29.4, 29.3, 26.7, 22.9, 22.2, 14.4; ^{19}F: −80.0 s.

Dielectric Spectroscopy. The temperature dependence of the ionic conductivity was measured using a Novocontrol broadband dielectric spectrometer in the frequency range of 10^{-1}−10^{7} Hz. The samples were placed between two stainless steel electrodes with a Teflon spacer (diameter of 12.3 mm and thickness of 1 mm) and loaded into a cryo-furnace. The cell was assembled in an argon atmosphere. Data were collected in steps of 10 K in the temperature range of 150 to −50 °C upon cooling within a nitrogen dry atmosphere. The DC conductivity was extracted as the low-frequency plateau in the frequency-dependent conductivity plot.

Differential Scanning Calorimetry. Measurements were performed on a TA Instrument Q1000. For each measurement, the sample was placed in a hermetically sealed aluminum pan (in an Ar-filled glovebox), and an empty pan was used as the reference. The samples were first cooled from 40 to −150 °C at a rate of 20 K/min, and the DSC traces were recorded during the subsequent heating scan up to 150 °C at a rate of 10 K/min within helium gas inert and dry environments. The Universal Analysis 2000 software (TA Instruments) was used to identify the thermal transitions. The glass transition temperatures were taken as the midpoint of the heat capacity change, whereas the melting points were taken as the minimum value of the endothermic peak of fusion.

Thermogravimetric Analysis. TGA was made using a Netzsch 209 TG F1 with alumina pans. Samples were prepared inside of a glovebox and transferred under argon to the instrument and exposed to air only immediately before the measurement for a maximum of approximately 5 s. During the measurements, a purge gas stream of 20 mL/s of N_2 was applied. The sample loading was 7−20 mg. The applied temperature program for decomposition was heating from RT to 400 °C at 5 K/min. Isotherms were measured by heating at 60 K/min to the target temperature and subsequently held for 16 h.

Infrared Spectroscopy. All experiments were performed on a Bruker Alpha spectrometer under an argon atmosphere. Spectra were recorded in attenuated total reflection (ATR) mode using a diamond crystal, in the region of 450−4000 cm^{-1}, averaging over 200 scans and with a resolution of 1 cm^{-1}.

dx.doi.org/10.1021/jz300752u | J. Phys. Chem. Lett. 2012, 3, 2114−2119

NMR Spectroscopy. Experiments were carried out with a Varian spectrometer at an operating proton frequency of 400 MHz (the ^{1}H frequency is 400.1 MHz, that of ^{13}C is 100.6 MHz, and the ^{19}F frequency is 376.5 MHz) at room temperature. ^{1}H and ^{13}C chemical shifts are referenced to the solvent as internal standards relative to TMS. ^{19}F spectra are referenced to an external stick with C_6F_6 dissolved in the corresponding deuterated solvent, referenced to −164.90 ppm. A $^{1}H-^{19}F/^{15}N-^{31}P$ 5 mm PFG PZT OneNMR probe (VT400NB 54 mm) was used for all experiments.

Diffusion NMR Spectroscopy. Experiments were recorded on a Varian spectrometer (the ^{1}H frequency is 500.1 MHz, and that for ^{19}F is 470.6 MHz) at 80 °C with a $^{1}H-^{19}F/^{15}N-^{31}P$ 5 mm PFG dual broad-band probe (VT 500 NB). The temperature was calibrated with ethylene glycol.[29] The experiments were performed on pure AAILs without any deuterated internal or external standard. The spectrometer was shimmed manually by looking at the shapes and heights of the NMR lines in the transformed proton spectra. A gradient-compensated stimulated echo pulse sequence with spin-lock and convection compensation was used,[30] z-gradients were employed, and 4−8 scans were acquired. For all experiments, a 25 s relaxation delay was applied to ensure full relaxation, a 4 ms gradient pulse duration and 300 ms diffusion delay were used, and the gradient strength was arrayed between 0 and 60 G cm^{-1} (15−20 steps). The diffusion coefficients were calculated using the data of H_2O in DMSO at 20 °C (9×10^{-10} m^2 s^{-1}).[31] All data analysis was performed using Varian VNMR 3.2beta. The VNMR DOSY processing program was used, and the diffusion data were obtained via integrating the corresponding peaks.

AUTHOR INFORMATION

Corresponding Author

*Fax: (+)46-31-772 2090. E-mail: patrik.johansson@chalmers.se.

Author Contributions

The manuscript was written through contributions of all authors. All authors have given approval to the final version of the manuscript.

Notes

The authors declare no competing financial interest.

ACKNOWLEDGMENTS

We would sincerely like to thank both the Swedish Research Council for Environment, Agricultural Sciences and Spatial Planning (FORMAS), the Swedish Research Council (VR), and the Swedish Energy Agency (STEM) for their generous funding.

ABBREVIATIONS

AAIL, anion amphiprotic ionic liquids; PIL, protic ionic liquid; EMIm, ethylmethylimidazolium; BMIm, butylmethylimidazolium; BMPyr, butylmethylpyrrolidinium; 8881N, trioctylmethylammonium; 4111N, butyltrimethylammonium; TFSAm, trifluoromethanesulfonamide; PEMFC, proton-exchange membrane fuel cell; DSC, differential scanning calorimetry; TGA, thermogravimetric analysis; DOSY, diffusion-ordered spectroscopy; TMS, tetramethylsilane; ATR, attenuated total reflection; PFG, pulsed field gradient

REFERENCES

(1) Wilkes, J. S. A Short History of Ionic Liquids—From Molten Salts to Neoteric Solvents. *Green Chem.* **2002**, *4*, 73−80.

(2) Greaves, T. L.; Drummond, C. J. Protic Ionic Liquids: Properties and Applications. *Chem. Rev.* **2008**, *108*, 206−37.

(3) Xu, W.; Angell, C. A. Solvent-Free Electrolytes with Aqueous Solution-Like Conductivities. *Science* **2003**, *302*, 422−425.

(4) Susan, M.; Noda, A.; Mitsushima, S.; Watanabe, M. Brønsted Acid−Base Ionic Liquids and Their Use As New Materials for Anhydrous Proton Conductors. *Chem. Commun.* **2003**, 938−939.

(5) Steele, B. C.; Heinzel, A. Materials for Fuel-Cell Technologies. *Nature* **2001**, *414*, 345−352.

(6) Yoshizawa, M.; Xu, W.; Angell, C. A. Ionic Liquids by Proton Transfer: Vapor Pressure, Conductivity, and the Relevance of ΔpK_a from Aqueous Solutions. *J. Am. Chem. Soc.* **2003**, *125*, 15411−15419.

(7) Ogihara, W.; Kosukegawa, H.; Ohno, H. Proton-Conducting Ionic Liquids Based upon Multivalent Anions and Alkylimidazolium Cations. *Chem. Commun.* **2006**, 3637−3639.

(8) Holbrey, J. D.; Reichert, W. M.; Tkatchenko, I.; Bouajila, E.; Walter, O.; Tommasi, I.; Rogers, R. D. 1,3-Dimethylimidazolium-2-carboxylate: The Unexpected Synthesis of an Ionic Liquid Precursor and Carbene−CO_2 Adduct. *Chem. Commun.* **2003**, 28−29.

(9) Smiglak, M.; Holbrey, J. D.; Griffin, S. T.; Reichert, W. M.; Swatloski, R. P.; Katritzky, A. R.; Yang, H.; Zhang, D.; Kirichenko, K.; Rogers, R. D. Ionic Liquids *via* Reaction of the 1,3-Dimethylimidazolium-2-carboxylate with Protic Acids. Overcoming Synthetic Limitations and Establishing New Halide Free Protocols for the Formation of ILs. *Green Chem.* **2007**, *9*, 90−98.

(10) Tokuda, H.; Hayamizu, K.; Ishii, K.; Susan, M. A. B. H.; Watanabe, M. Physicochemical Properties and Structures of Room Temperature Ionic Liquids. 1. Variation of Anionic Species. *J. Phys. Chem. B* **2004**, *108*, 16593−16600.

(11) Ohno, H.; Yoshizawa, M. Ion Conductive Characteristics of Ionic Liquids Prepared by Neutralization of Alkylimidazoles. *Solid State Ionics* **2002**, *155*, 303−309.

(12) Ignat'ev, N. V.; Welz-Biermann, U.; Kucheryna, A.; Bissky, G.; Willner, H. New Ionic Liquids with Tris(perfluoroalkyl) Trifluorophosphate (FAP) Anions. *J. Fluorine Chem.* **2005**, *126*, 1150−1159.

(13) Pitawala, J.; Matic, A.; Martinelli, A.; Jacobsson, P.; Koch, V.; Croce, F. Thermal Properties and Ionic Conductivity of Imidazolium Bis(trifluoromethanesulfonyl)imide Dicationic Ionic Liquids. *J. Phys. Chem. B* **2009**, *113*, 10607−10610.

(14) Martinelli, A.; Matic, A.; Jacobsson, P.; Börjesson, L.; Fernicola, A.; Scrosati, B. Phase Behaviour and Ionic Conductivity in Lithium Bis(trifluoromethanesulfonyl)imide-Doped Ionic Liquids of the Pyrrolidinium Cation and Bis(trifluoromethanesulfonyl)imide Anion. *J. Phys. Chem. B* **2009**, *113*, 11247−11251.

(15) Giernoth, R.; Bankmann, D. Application of Diffusion-Ordered Spectroscopy (DOSY) as a Solvent Signal Filter for NMR in Neat Ionic Liquids. *Eur. J. Org. Chem.* **2005**, *2005*, 4529−4532.

(16) Ueki, T.; Watanabe, M. Macromolecules in Ionic Liquids: Progress, Challenges, and Opportunities. *Macromolecules* **2008**, *41*, 3739−3749.

(17) Noda, A.; Susan, M. A. B. H.; Kudo, K.; Mitsushima, S.; Hayamizu, K.; Watanabe, M. Brønsted Acid−Base Ionic Liquids as Proton-Conducting Nonaqueous Electrolytes. *J. Phys. Chem. B* **2003**, *107*, 4024−4033.

(18) Reichardt, C.; Welton, T. *Solvents and Solvent Effects in Organic Chemistry*; Wiley-VCH Verlag GmbH: Weinheim, Germany, 2011.

(19) Cukierman, S.; et al. Grotthuss! and Other Unfinished Stories. *Biochim. Biophys. Acta* **2006**, *1757*, 876−885.

(20) Agmon, N. The Grotthuss Mechanism. *Chem. Phys. Lett.* **1995**, *244*, 456−462.

(21) Behrend, E.; Haas, A. Trifluormethyl-schwefel-stickstoff-verbindungen. IX. Trifluormethansulfonamide. *J. Fluorine Chem.* **1974**, *4*, 99−106.

(22) Zhang, S.; Sun, N.; He, X.; Lu, X.; Zhang, X. Physical Properties of Ionic Liquids: Database and Evaluation. *J. Phys. Chem. Ref. Data* **2006**, *35*, 1475−1517.

(23) Bonhote, P.; Dias, A.; Papageorgiou, N.; Kuppuswamy, K.; Grätzel, M. Hydrophobic, Highly Conductive Ambient Temperature Molten Salts. *Inorg. Chem.* **1996**, *35*, 1168−1178.
(24) Wachter, P.; Schreiner, C.; Schweiger, H.-G.; Gores, H. J. Determination of Phase Transition Points of Ionic Liquids by Combination of Thermal Analysis and Conductivity Measurements at Very Low Heating and Cooling Rates. *J. Chem. Thermodyn.* **2010**, *42*, 900−903.
(25) Belieres, J.-P.; Angell, C. A. Protic Ionic Liquids: Preparation, Characterization, and Proton Free Energy Level Representation. *J. Phys. Chem. B* **2007**, *111*, 4926−4937.
(26) Yasaka, Y.; Wakai, C.; Matubayasi, N.; Nakahara, M. Water as an In Situ NMR Indicator for Impurity Acids in Ionic Liquids. *Anal. Chem.* **2009**, *81*, 400−407.
(27) Trepka, R. D.; Belisle, J. W.; Harrington, J. K. Acidities and Partition Coefficients of Fluoromethanesulfonamides. *J. Org. Chem.* **1974**, *39*, 1094−1098.
(28) Degen, G.; Stock, C. Method for Producing Imidazolium Salts. U.S. Patent Application 10/520,800 2008.
(29) Bernal, J. D.; Fowler, R. H. A Theory of Water and Ionic Solution, with Particular Reference to Hydrogen and Hydroxyl Ions. *J. Chem. Phys.* **1933**, *1*, 515−548.
(30) Raiford, D. S.; Fisk, C. L.; Becker, E. D. Calibration of Methanol and Ethylene Glycol Nuclear Magnetic Resonance Thermometers. *Anal. Chem.* **1979**, *51*, 2050−2051.
(31) Jerschow, A.; Müller, N. Suppression of Convection Artifacts in Stimulated-Echo Diffusion Experiments. Double-Stimulated-Echo Experiments. *J. Magn. Reson.* **1997**, *125*, 372−375.